Electrode Erosion and Lifetime Performance of a Triggered, Corona-stabilized Switch in SF_6 at a Repetition Rate of 1 kHz

John M. Koutsoubis
Department of Electrical Engineering
Technological Educational Institute (TEI) of Central Greece in Chalkis
Psahna GR 34400, Euboea, Greece

Katerina Thoma
Department of Mining Engineering and Metallurgy
National Technical University of Athens (NTUA)
9 Iroon Polytechniou Street, Zografou GR 15780, Greece

and **Scott J. MacGregor**
Institute for Energy and Environment, Department of Electronic and Electrical Engineering
University of Strathclyde
204 George Street, Glasgow G1 1XW, Scotland, UK

ABSTRACT

This paper describes the work undertaken to investigate the electrode erosion and lifetime performance of an electrically triggered, corona stabilized (TCS) switch. The switch, which had a rod-plane geometry, was filled with SF_6 at a pressure of 0.8 bar (1.0bar = 100kPa) absolute and was operated at a pulse repetition frequency (PRF) of 1kHz. The erosion rates of anode and cathode electrode materials such as elkonite (a copper tungsten composite), brass, aluminum and two types of stainless steel was measured, and their surfaces were studied optically, photographed and chemically analyzed. The erosion rate of the anode (rod) electrode materials ranged from 21.39 x 10^{-6} cm^3C^{-1} for elkonite to 60.4 x 10^{-6} cm^3C^{-1} for brass, whilst a cathode (trigger disc) erosion rate as high as 51.23 x 10^{-6} cm^3C^{-1} for aluminum was measured. The lifetime of the TCS switch was experimentally determined for each of the electrode material tested, and was found to be inversely proportional to the erosion rate of the rod electrode. The electrode surface morphology and the gas-electrode compound distribution have also been evaluated to address the erosion mechanism in effect. Additionally, the influence of rod electrode surface conditions and gas deterioration has been investigated in respect to the performance and operational behavior of the TCS switch.

Index Terms — **Corona stabilization, high-pressure plasma closing switches, gas discharges, electrode erosion, electronegative gases.**

1 INTRODUCTION

CORONA stabilization is a novel technique used to improve the high-pulse repetition frequency (PRF) performance of high-pressure plasma closing switches while retaining the excellent switching characteristics, simplicity and cost efficiency of the conventional spark gap [1]. This is achieved by utilising the phenomenon of corona-stabilized breakdown, where the presence of a corona discharge after the application of a slow-rising or DC charging voltage delays and effectively inhibits premature breakdown of the gap. The stabilizing effect relies upon the space charge generated from the corona discharge, which de-couples the HV electrode of the switch from the rest of the gap, thus permitting the neutral gas density in the inter-electrode area to recover freely [1, 2].

In order to achieve an efficient stabilizing corona discharge, the switch geometry must be configured in such a way that a highly non-uniform electric field is produced in front of the HV electrode. In addition, the gas that will act as a switching medium must have strong electronegative properties. Both of these requirements are essential for the high-PRF performance of the switch because they are closely associated to the de-coupling (formative) time between the establishment of the corona discharge and breakdown of the switch. Generally, the

Manuscript received on 11 November 2015, in final form 8 April 2016, accepted 12 April 2016.

higher the field non-uniformity at the HV electrode, the longer the delay time between the establishment of the corona discharge and breakdown [3]. The same applies with strong electronegative gases such as SF_6, Freons and their mixtures compared to gases with weaker electronegative properties such as air [4, 5]. A previous study has shown that the use of SF_6 has improved the burst-mode high-PRF capabilities of a triggered corona stabilized (TCS) switch by a factor of more than three compared to that obtained with synthetic air [5], a result primarily attributed to the highly efficient corona stabilization process in SF_6. When this is combined with the superior thermo-physical properties [6] of SF_6, the latter is a preferred choice for high-PRF switching applications. At the same time however, this can introduce lifetime limitation effects due to enhanced electrode erosion [7].

The electrode erosion mechanism in corona stabilized switches, especially at high repetition rates, is a highly complicated process, and cannot be readily explained by conventional spark gap erosion studies that concern switches having large mass and sparking area electrodes [8]. This is due to the fact that the non-uniform field electrode of a corona stabilized switch usually exhibits a low mass, as well as a very small active discharge area. The net result is that the electrode tip is subjected to very high average temperatures during high-PRF operation leading to the formation of various gas-electrode compounds that play a dominant role on the erosion mechanism [7, 9]. In case SF_6 is used as a switching gas, in the presence of an electric discharge it dissociates to produce a large number of molecular, atomic and ionic species [10]. These, by virtue of their extremely reactive nature, are particular efficient in eroding the non-uniform field electrode of a corona stabilized switch, thus limiting the usable lifetime of the device. Other lifetime limiting parameters arise from the fact that corona stabilized switches are normally used as gas-sealed devices where no gas flow or frequent purging takes place during their operation. Due to this reason, accumulated effects such as gas deterioration (poisoning), deteriorated gas-electrode reactions and pollution of the switch insulation surfaces from sparking debris and corona by-products can act synergistically to alter the breakdown voltage levels of the device. This consequently degrades the operational consistency of the device by introducing pre-firing or misfiring periods during a long switch run [9].

This paper reports on the work undertaken to investigate the erosion characteristics of five different types of electrode materials and experimentally determine the lifetime performance of a TCS switch, with SF_6 at a PRF of 1 kHz. In addition, the effect of the charging voltage polarity has also been investigated, as this has been found to play an important role on the electrode erosion mechanism. Finally, the effects of non-uniform field electrode modification and switching gas deterioration on the operational performance of the switch have also been investigated.

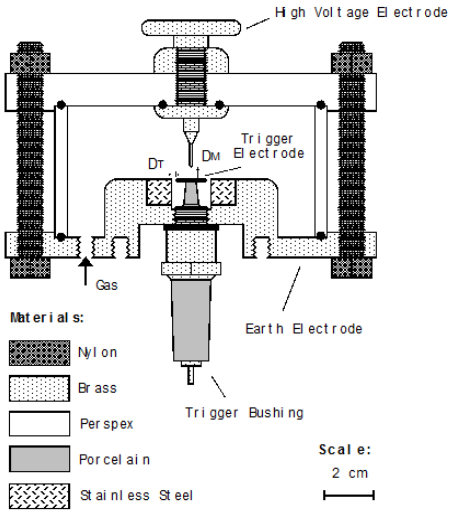

Figure 1. Schematic diagram of the TCS switch.

2 EXPERIMENTAL

The schematic of the TCS switch used in this investigation is shown in Figure 1. It consisted of a hemispherically capped rod HV electrode with a nominal radius of 0.5mm (±10%) opposite to an earthed plane electrode. The plane electrode has an axial bore in which a disc shaped electrode is positioned. The main gap (D_M), formed between the rod/trigger disc electrodes, and the annular trigger gap (D_T), formed between the trigger disc/earthed plane electrodes, were set to 5mm and 3.5mm respectively throughout the tests. In order to study the erosion rates of five different electrode materials at 1kHz, and consequently the lifetime of the TCS switch, ten identical rod/trigger disc electrode sets were constructed (two sets of each material). The materials used for their construction were brass (CZ121M), elkonite (Cu28/W72), aluminum (BS4300/5-2011) and two types of stainless steel (303-S31 and 316-S31).

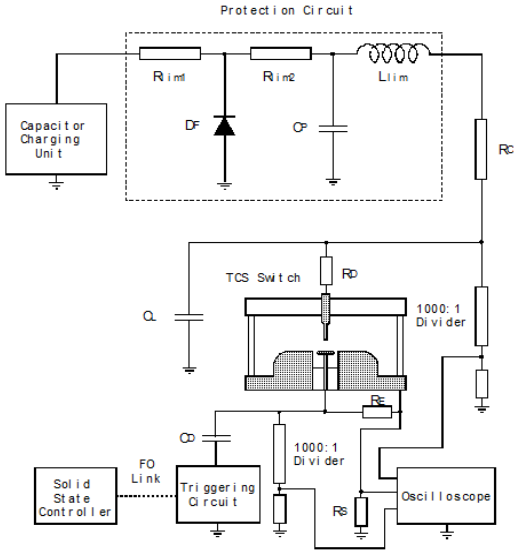

Figure 2. Experimental set-up used for the TCS switch electrode erosion and lifetime tests.

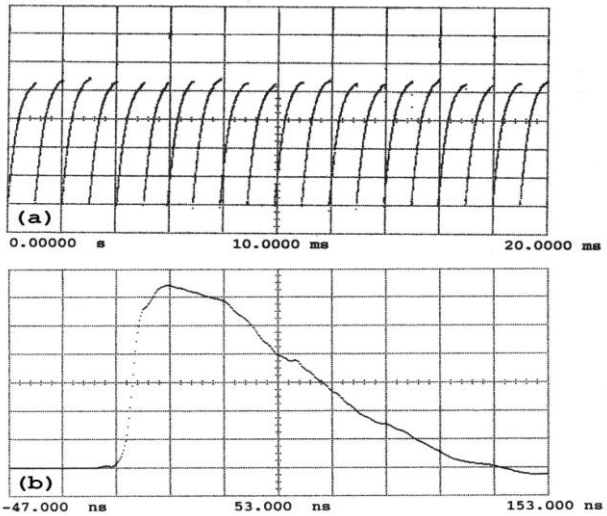

Figure 3. Typical oscilogram recordings with a positive charging voltage polarity. (a) Voltage across the TCS switch (5kV/div); Timebase: 2ms/div. (b) Discharge current through the TCS switch (150A/div); Timebase: 20ns/div.

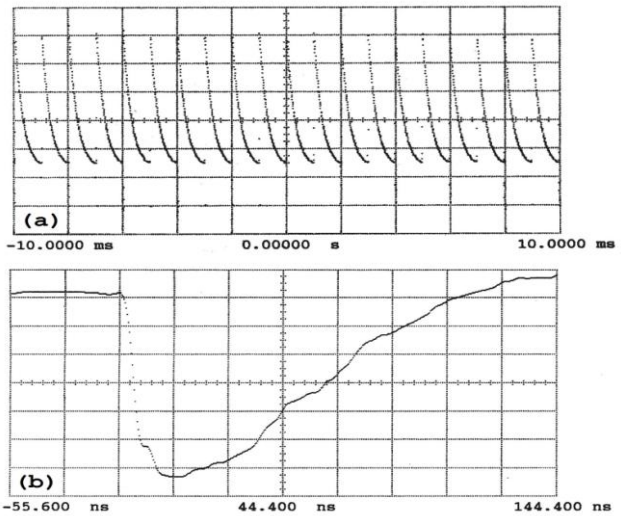

Figure 4. Typical oscilogram recordings with a negative charging voltage polarity. (a) Voltage across the TCS switch (5kV/div); Timebase: 2ms/div. (b) Discharge current through the TCS switch (150A/div); Timebase: 20ns/div.

The earthed plane electrode was made from brass with a stainless steel sleeve around the axial bore (Figure 1) to minimize erosion on the earth side of the trigger gap. A high-ohmic resistor (R_E) having a value of 5.1 MΩ was connected across the trigger gap to ensure that the trigger electrode stays near earth potential during charging of the main gap. For all of the experimental work described in this study, the TCS switch was filled with SF_6 gas at a pressure of 0.8 bar (80 kPa) absolute. A more detailed description of the design and operational characteristics of the TCS switch can be found elsewhere [11, 12].

The experimental arrangement used in the investigation can be seen in Figure 2. The 3.0 nF/40 kV load capacitor (C_L) connected across the TCS was charged to 22 kV throughout the study, which resulted to in an energy of 0.73 J or a charge of 66 μC transferred to the load during each switch closure. Since this investigation was conducted at high average power levels in a continuous mode of operation, an ALE 202L, 40 kV/2 kW capacitor charging unit together with a 106 kΩ/2 kW wire-wound charging resistor (R_C) was utilized. The value of the charging resistor was chosen to result in a charging constant three times smaller than the operating repetition rate (PRF ≈ ⅓ τ). Figures 3a and 4a show the charging voltage waveforms across the TCS switch with a positive and a negative polarity respectively. In order to protect the power supply from voltage reversals during the discharge of the load capacitor, a protection circuit was also included in the test circuit. The TCS switch was triggered by means of a battery powered trigger circuit, controlled by a solid state controller via a fiber optic link [11]. The trigger pulse had an opposite polarity and a magnitude equal to the charging voltage of the switch ($V_{TR} \cong 100\% V_{CH}$). In order to distinguish the different erosion rates between anode and cathode materials, an aqueous $CuSO_4$ resistor (R_D) with a value of 11 Ω was connected in series with the TCS switch to critically damp the discharge current [9]. The current was monitored with an in-house, high-speed coaxial shunt having a resistance of 12.5 mΩ (R_M).

As shown in Figures 3b and 4b, the discharge current had a unipolar waveform and was measured to have a peak value of 1kA with a rate of rise of 52 $kA\mu s^{-1}$. The charging and trigger voltages of the TCS switch were measured with two North Star PVM-1, 1000:1 resistive-capacitive (RC) compensated HV dividers. The output signals from the current shunt and the HV dividers were viewed and recorded on a Hewlett Packard 54112D, 100MHz digitizing oscilloscope.

Prior to testing, the rod and trigger disc electrodes were polished with a fine rouge paste and a soft cloth, rinsed with absolute alcohol and weighed with a Cahn TA4100 digital analytical balance having an accuracy of ±100 μg. After the electrodes were positioned, the switch was filled with SF_6 at the required pressure and sealed. The TCS switch was then operated continuously for 30 s at a PRF of 1 kHz. After the termination of this operating period, the switch was evacuated, refilled with new gas, and operated for a further 30-second period. These start-stop gas-changeover cycles were repeated continuously, until erosion effects on the rod electrode prevented the TCS switch from operating properly at the given test conditions (gas pressure, charging and trigger voltage). The end of the TCS switch lifetime was verified after a ≈20% misfire rate occurred with new gas close to the middle of an operation period. For each material type, the electrode erosion and lifetime tests were repeated using the second rod/trigger disc electrode set in order to confirm the results and minimize the measurement errors.

After the termination of the tests, the electrodes were examined and photographed by means of 10x–60x optical microscope and a Zenith 122 35mm reflex camera, and chemically analyzed with a Jeol JSM6100 scanning electron microscopy (SEM) facility equipped with a Noran Instruments (Tracor Europe) energy dispersive X-ray spectrometer (EDS). Finally, they were cleaned with alcohol and weighed in order to determine the electrode material loss due to the switching operation of the TCS switch.

3 RESULTS

3.1 ELECTRODE EROSION CHARACTERISTICS – SWITCH LIFETIME

The erosion rates (mean values) of the five materials tested for both rod (anode) and trigger disc (cathode) can be seen in Figure 5. The lowest rod (anode) erosion rate was displayed by elkonite (21.39 x 10^{-6} cm^3C^{-1}) followed by aluminum (34.91 x 10^{-6} cm^3C^{-1}), which exhibited a markedly higher erosion rate. The stainless steel (SSt) anodes showed moderately higher erosion rates than aluminum, with values of 39.48 x 10^{-6} cm^3C^{-1} for SSt303 and 39.81 x 10^{-6} cm^3C^{-1} for SSt316 respectively. Finally the brass rod (anode) electrode displayed an erosion rate of 60.4 x 10^{-6} cm^3C^{-1}, which was by far the largest measured of all of the materials tested in SF_6. The trigger disc (cathode) electrodes showed in general, a moderately small variation, ranging from 23.2 x 10^{-6} cm^3C^{-1} for elkonite, 28.77 x 10^{-6} cm^3C^{-1} for SSt303, 30.3 x 10^{-6} cm^3C^{-1} for SSt316 to 34.94 x 10^{-6} cm^3C^{-1} for brass. The exception was aluminum, which showed an erosion rate almost two times higher (51.23 x 10^{-6} cm^3C^{-1}) than the other cathode materials.

In order to investigate the effect of the charging voltage polarity on electrode erosion, a supplementary lifetime test was performed with negative charging voltage under identical experimental parameters. For this reason, two additional rod/trigger disc electrode sets were fabricated from brass. As shown in Figure 6, the erosion rate of the negative brass rod (cathode) electrode was found to be lower by about a factor of four (15.5 x 10^{-6} cm^3C^{-1}) compared to the value obtained with the positive charging voltage test. At the same time, the erosion rate of the positive trigger disc (anode) increased by about 35% (47.19 x 10^{-6} cm^3C^{-1}). In Figure 7, the lifetime of the TCS switch is plotted against the erosion rates of the different electrode materials used. The switch lifetime data presented in this graph have been normalized to account for small differences in the radii of the rod electrodes. The normalized lifetime data were derived from the calculation of the normalized total charge transferred through the switch for each material type, using the average length eroded off the rod electrodes following the termination of the tests. This length was found to be 1.01 mm ±10% for all materials with positive voltage, and 1.4 mm ±10% for negative voltage.

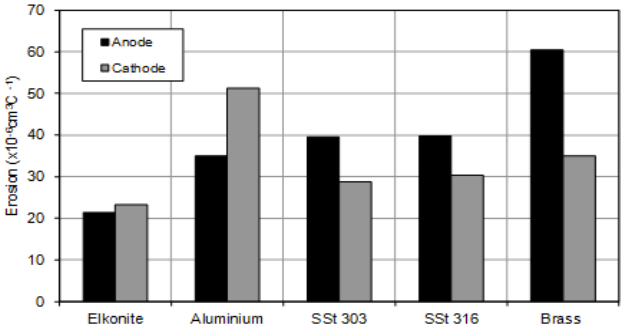

Figure 5. Erosion of the anode (rod) and cathode (trigger disc) of the TCS switch. Material types are displayed in the order of increasing anode erosion.

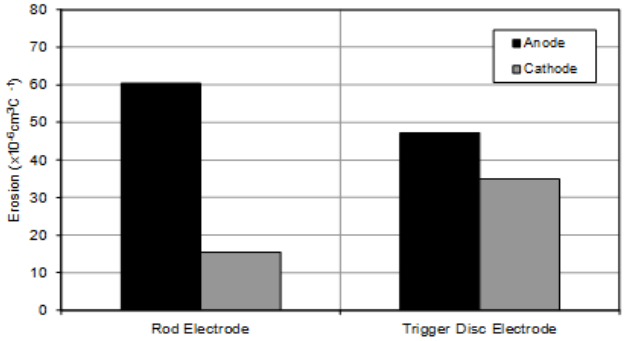

Figure 6. The effect of the charging voltage polarity on the erosion rates of the brass rod and trigger disc electrodes. Note that the positive electrode always exhibits a higher erosion rate than the negative electrode, regardless of its shape.

From Figure 7, a dependency between the erosion rate of the rod electrodes and switch lifetime is evident, with the higher the erosion rate of a certain material, the lower the resulting switch lifetime. Thus, the highest switch lifetime was exhibited by the elkonite rod electrode (0.57 x 10^6 shots), which was followed by aluminum, SSt303 and SSt316 with corresponding lifetimes of 0.35 x 10^6, 0.306 x 10^6 and 0.306 x 10^6 shots respectively. Finally, the performance of the brass rod (Brass +) electrode was not impressive, displaying a lifetime of only 0.2 x 10^6 shots. This poor performance was as expected, since the brass rod electrode exhibited the higher erosion rate of all materials tested.

In the case of the supplementary experiment that utilized a negatively charged brass rod HV electrode, it was found that the polarity of the charging voltage played a role on the lifetime performance of the TCS switch. As seen in Figure 7, when the brass rod electrode was negatively charged (Brass -), the switch exhibited a lifetime of 1.05 x 10^6 shots, which represented a fivefold increase (0.2 x 10^6 shots) over the positively charged brass rod electrode (Brass +).

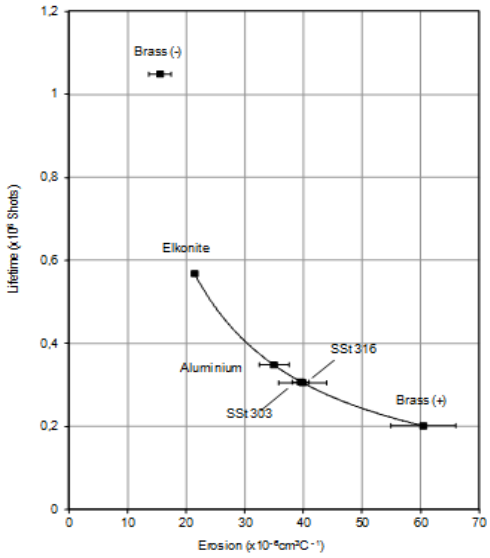

Figure 7. Anode erosion rates against the TCS switch lifetime of the five electrode materials tested.

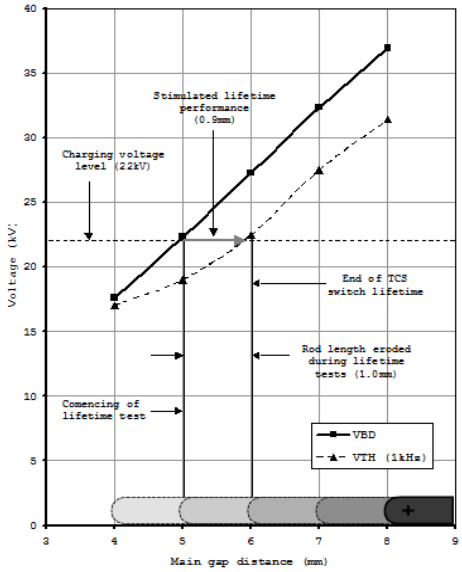

Figure 8. V/D_M (voltage/main gap distance) characteristics of the TCS switch displaying the simulated lifetime performance of the device (grey colored arrow) at a charging voltage of +22 kV.

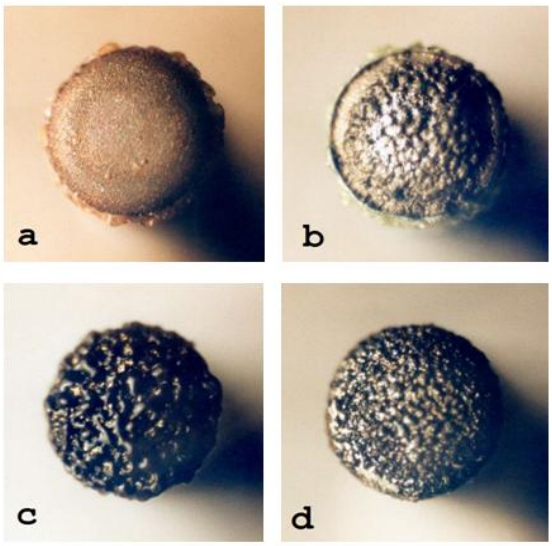

Figure 9. End-on photographs of the rod (anode) electrodes of the TCS switch with a positive charging voltage. The rod tips are illuminated from the left-hand side of the photographs: (a) elkonite, (b) stainless steel 303, (c) brass, (d) aluminum.

This significant increase in the switch lifetime is the net result of the following reasons. The first is due to the much lower erosion rates exhibited by the negatively charged brass rod electrode (Figure 7), which is directly related to the lifetime performance of the device. Secondly, from the average length eroded off the rod electrodes, it is evident that with a negative charging voltage, the switch can be operated at a far lower triggering threshold. Figure 8, displays the V/D_M (voltage/main gap distance) characteristics of the TCS switch, by which the lifetime performance of the device can be estimated at a PRF of 1 kHz. This is achieved by varying the main gap distance of the switch from 4-8 mm in steps of 1 mm, which simulates the erosion of the rod electrode with increasing shot number, and measuring the self-breakdown and triggering threshold voltage levels. Moreover, with a positive charging voltage of 22 kV, the rod electrode could be eroded by about 1mm before the switch reached the end of its lifetime, a value that is in agreement with the simulated lifetime performance graph shown in Figure 8. However, in the case of the negative charging voltage and under similar experimental parameters, this length was found to have a value of 1.4mm. This means that, regardless of the electrode material used, for identical charging and triggering voltage levels, a negative charging voltage operated switch can be triggered at a larger main gap spacing than the positive polarity, which consequently extends the switch lifetime.

3.2 ELECTRODE SURFACE MORPHOLOGY

In Figure 9, the end-on photographs of the rod (anode) electrodes are shown following the termination of the lifetime tests. Due to the similar appearance of the surface conditions of the electrodes made from stainless steel SSt303 and SSt316, only the photographs of the former type (SSt303) are presented in this section. Generally, all the rod electrodes developed a flattened tip profile with their surfaces more or less covered by protrusions having various sizes.

As seen in Figure 9a, the elkonite rod tip exhibits a reasonably smooth and lightly pitted discharge area. Apart from a few large-sized protrusions (≈20μm) with a distinct reddish color, the rest of the discharge area has a grainy-like appearance. In contrast to elkonite, the stainless steel (SSt303/SSt316) rod electrode tips (Figure 9b) displayed a much more structured surface with a smaller central sparking area. This central area was covered with moderately large sized (80μm) blunt protrusions with a distinct metallic appearance. The surfaces of brass and aluminum rod electrodes showed a very similar morphology, with their rod tips almost fully covered with dark colored protrusions. These protrusions on the brass rod tip (Figure 9c) have a characteristic glossy appearance, with sizes up to about 100μm and a black color. The aluminum rod electrode (Figure 9d) is covered with medium to small sized (50-10μm), dark-grey protrusions.

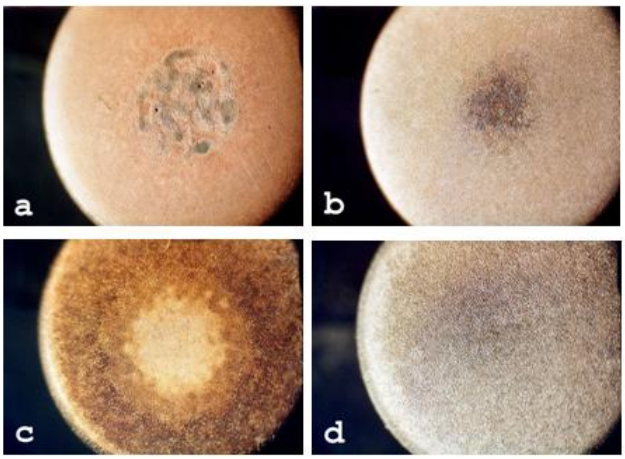

Figure 10. Face-on photographs of the trigger disc (cathode) electrodes of the TCS switch with a positive charging voltage. The disc electrodes are illuminated from the left-hand side of the photographs: (a) elkonite, (b) stainless steel 303, (c) brass, (d) aluminum.

On the periphery of the sparking region, particularly for elkonite and SSt303/316 rod electrodes and to a lesser extent for brass, there is a zone of rough material that has a particular crystal-like appearance. This was not observed on the aluminum rod electrode. The predominant color of the material in this zone is pinkish-white for elkonite and brass electrodes, whilst for the SSt303/316 electrodes it is greenish-white. This zone, which extends for about 1mm along the length of the rod electrodes, is composed mainly of accumulated gas-electrode compounds [13].

The conditions of the surface of the trigger disc (cathode) electrodes can be seen in Figure 10. Generally, on all of the trigger disc electrodes, a central region can be observed, with its diameter, color, shading and intensity depending upon the electrode material. This central discharge area is very clearly defined on the elkonite and brass trigger disc electrodes, whilst this is less defined on the stainless steel and aluminum electrodes. In contrast to the rest of its surface, the elkonite trigger disc (Figure 10a) exhibits a severely pitted central region, full of flat grey colored areas and deep pores, with the latter having diameters up to 0.6mm. The stainless steel, brass and aluminum trigger disc electrodes are uniformly pitted up to their edges, with brass displaying a central region much lighter in color than its surrounding area (Figure 10c). The opposite can be seen for the stainless steel electrodes (Figure 10b), which show a small central region that is much darker than its surroundings. In the case of aluminum (Figure 10d), this region is only defined by the slightly coarser pitting markings towards the centre of the trigger disc electrode.

The brass electrodes of the TCS switch tested with the negative charging voltage, displays a different surface morphology to that found with the positive charging voltage configuration. As seen in Figure 11a, the brass rod (cathode) electrode exhibits a fairly smooth and shiny surface that is uniformly covered by relatively small sized protrusion (≈20μm). On the other hand, the brass trigger electrode (anode) seen in Figure 11b, displays a severely damaged surface with extensive erosion markings and globule-like protrusions up to the edge of the disc. The extent of this damage is the result of the combined effect of sparking and corrosive attack, as indicated by the presence of black colored substances on the trigger disc surface.

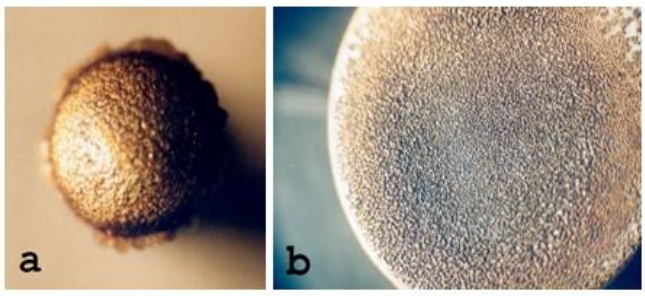

Figure 11. Photographs of the brass electrodes of the TCS switch with a negative charging voltage. The electrodes are illuminated from the left-hand side of the photographs. (a) End-on view of the rod (cathode) electrode. (b) Face-on view of the trigger disc (anode) electrode.

3.3 ELECTRODE SURFACE SEM/EDS CHEMICAL ANALYSIS

Following completion of the switch lifetime tests in SF_6, the surfaces of the rod and trigger disc electrodes were examined with a scanning electron microscope (SEM) facility equipped with an energy dispersive X-ray spectrometer (EDS). This examination was carried out to gain information on the relative concentrations of residual gas-electrode by-products (metal fluorides and sulfides) that were present on and around the discharge areas of the switch electrodes. The SEM/EDS analysis was also useful in detecting alterations in the ratio of the constituent metals, due to heat-driven segregation effects. In addition to the chemical analysis, the SEM facility was utilized to obtain high-resolution images of the discharge areas.

Table 1. Fluorine (F) and sulfur (S) relative concentrations detected with the EDS X-ray spectrometer on the discharge areas of the rod electrodes.

Rod Electrode Material	Centre		Periphery	
	F	S	F	S
Elkonite	0%	4.6%	-	-
Aluminum	14%	2.2%	-	-
Stainless Steel (303)	0-11.4%	1.3%	17.3%	1.1%
Stainless Steel (316)	0-7.9%	1.1%	31.5%	1.1%
Brass (+)	11.4%	6%	-	-
Brass (−)	5%	2.9%	-	-

Initially, all the switch electrodes were imaged face-on at a low magnification (85x for the rods and 12x for the trigger discs), whilst discharge areas that showed particular interest were imaged at higher magnifications (500x for the rods and 1000x for the trigger discs). During the high-magnification image capturing process, these areas were additionally analyzed for their chemical composition. Because the EDS microanalysis is not capable of producing reliable chemical analysis results when fluorine (Z=9) is included in the computation algorithm, the relative concentrations of the various elements detected on the electrodes were determined indirectly. This was achieved by comparing the x-ray peak count value of a specific emission line produced by a given element, to the total count number recorded in the chemical analysis graph [14]. Since this procedure produces simple emission line count ratios that have not been corrected for atomic number, absorption and x-ray florescence (ZAF) effects [15], the relative concentrations presented in this part of the study should be treated as indicative and not quantitative information.

Table 1 displays the relative concentrations of fluorine (F) and sulfur (S) compounds detected on the discharge areas of the rod electrodes. The figures quoted for each element are mean values from 2-3 different EDS chemical analysis measurements of the specific area under examination. As shown in Figures 12a-12b, the elkonite rod tip has a distinct granular appearance with only moderate concentrations of sulfur compounds detected, whilst on the periphery of the electrode there is an intense bright region consisting of the remains of the debris zone.

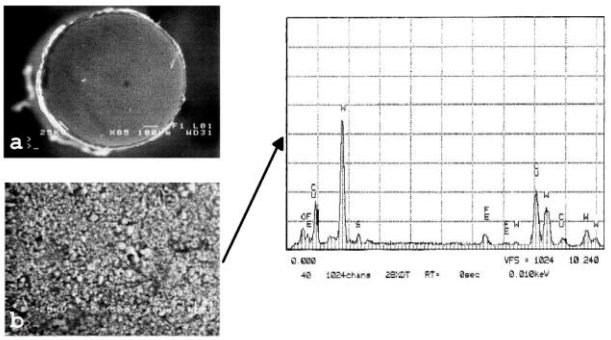

Figure 12. SEM images of the elkonite rod electrode (anode) of the TCS switch with a positive charging voltage. (a) Entire electrode view at 85x. (b) High-power view of the centre of the electrode at 500x and associated EDS X-ray peak graph.

It should be noted that generally a dark-colored region on a SEM image indicates a mostly metallic (conducting) surface, whilst bright-colored areas highlight chemical compound (insulating) deposits. In contrast to elkonite, the aluminum rod tip exhibited a relatively high fluoride content, which is generally representative of the rest of the examined rod electrode materials. In case of the stainless steel 303 and 316 electrodes, the central region displayed a much lower fluoride concentration than the periphery of the rod tips. It is worth noting here that the peripheral areas showed a substantial decrease in all the constituent elements of stainless steel. The sulfide compounds on the other hand, did not show the large variation displayed by the fluorides, as their concentration was very small throughout rod tip surfaces.

The brass electrodes had a special interest for this investigation, since this was the only material tested with both positive and negative charging voltages. On the discharge area of the positively charged brass rod (Figure 13a-13b), considerable amounts of fluorides and sulfides were detected, whilst on the negatively charged rod, these compounds were detected at concentrations reduced by about 50%. Apart from this, and regardless of the charging voltage polarity, zinc was significantly depleted from the discharge areas whilst, a moderate removal of copper was observed only from the positively charged electrode at a level much smaller than that for zinc.

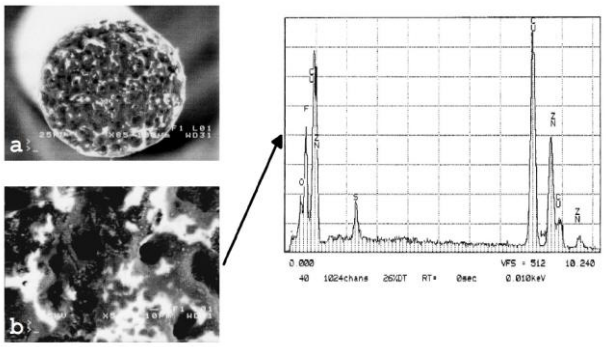

Figure 13. SEM images of the brass rod electrode (anode) of the TCS switch with a positive charging voltage. (a) Entire electrode view at 85x. (b) High-power view of the centre of the electrode at 500x and associated EDS X-ray peak graph.

Table 2. Fluorine (F) and sulfur (S) relative concentrations detected with the EDS X-ray spectrometer on the discharge areas of the trigger disc electrodes.

Trigger Disc Electrode Material	Centre		Periphery	
	F	S	F	S
Elkonite	0.8%*	2.9%†	20.6%	0%
Aluminum	9.5%	0.4%	4.4%	0.6%
Stainless Steel (303)	0%	6.7%	0%	1%
Stainless Steel (316)	0%	9.0%	0%	3.5%
Brass (+)	1.3%	1.4%	4.9%	1.1%
Brass (−)	19.5%	1.8%	21.4%	1%

*Dark colored regions †Light colored regions

Table 2 displays the relative concentrations of fluorine (F) and sulfur (S) compounds detected on the discharge areas of the trigger disc electrodes. Generally, on the surfaces of the trigger discs, two concentric regions can be identified, which can be distinguished by their different structure as well as their chemical composition.

The elkonite trigger disc displays the most complex distribution of gas-electrode compounds, with fluorine and sulfur compounds preferentially deposited on different areas of the electrode. As shown in Figures 14a-14b, on the central discharge region only small to moderate amounts of sulfur was detected on the light colored areas, whilst fluorine was detected only in trace amounts on the dark colored areas. The outer part of the elkonite trigger disc is dominated only by fluorine compounds, with its distribution being constant throughout this area except at the electrode edge, where it was detected in high concentrations (Figure 14c). Furthermore, whilst tungsten was found to predominate on the sulfur rich central discharge area, copper was detected in abundant quantities on the dark colored sites as well as on the fluorine rich outer regions.

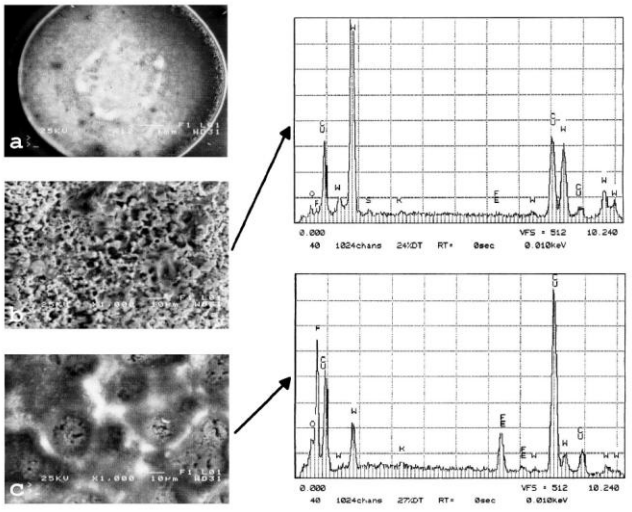

Figure 14. SEM images of the elkonite trigger disc electrode (cathode) of the TCS switch with a positive charging voltage. (a) Entire electrode view at 12x. (b, c) High-power view of the centre and periphery of the electrode at 1000x and associated EDS X-ray peak graphs.

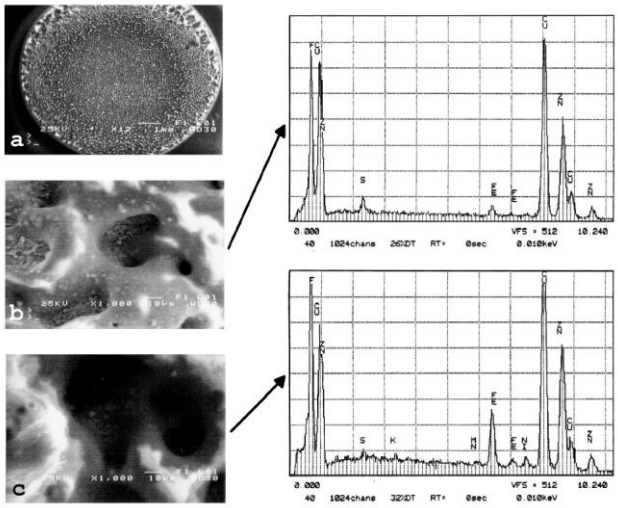

Figure 15. SEM images of the brass trigger disc electrode (anode) of the TCS switch with a negative charging voltage. (a) Entire electrode view at 12x. (b, c) High-power view of the centre and periphery of the electrode at 1000x and associated EDS X-ray peak graphs.

The aluminum trigger disc displayed an extensive central area, which displayed high concentrations of fluorine compounds. On the other hand, sulfur compounds were found only in trace amounts, showing a more or less constant distribution across the disc surface. On both the stainless steel (303/316) trigger disc electrodes the EDS chemical analysis detected sulfur compounds in moderate to high concentrations only at the central discharge region. The absence of fluorides should be treated with caution however, since their detection was hampered by the La-shell emission line of iron (0.71 keV), which falls very close to the Ka-shell line of fluorine (0.68 keV) [14].

Finally, on the central region of the brass trigger disc (cathode) tested with a positive charging voltage, both fluorine and sulfur compounds were detected in small concentrations with the latter being constant at this level throughout the surface of the electrode. On the contrary, the brass trigger disc tested with a negative charging voltage (anode) displayed a surface uniformly covered with fluorine compounds in abundant concentrations – the largest found on any of the electrodes examined (Figures 15b-15c). In case of the constituent metals of brass, both the cathode and anode trigger discs displayed a similar behavior compared to the brass rod electrodes (extensive zinc removal), as well as copper depletion from the positively charged electrode.

4 DISCUSSION

In high-duty (high-charge transfer per shot) spark gaps, the erosion mechanism is dominated by the processes of electrode material melting and vaporisation, as well as the ejection of liquid metal from the discharge site [8]. In lower-duty switches, the gas-electrode chemistry enhances the erosion mechanism, especially when SF_6 is used as a switching gas [13, 16]. The high temperatures developed during spark discharge can dissociate SF_6 resulting in a large number of highly reactive ionic species. The nature, population and ionisation state of these dissociated species is strongly dependent on the maximum plasma temperature as well as on the arc-cooling time [17]. Generally, over the temperature range from 3000 to 12000 K, the most abundant species found in a decaying spark plasma are fluorine and sulfur ions [17, 18], which react with the electrode surface to form fluorides and sulfides. This is an additional factor that makes the erosion mechanism more efficient in SF_6 compared to air, due to the fact that the majority of metal fluorides as well as some metal sulfides are known to be volatile or decompose readily at temperatures higher than 800-1000 °C. Since most of these compounds do not act in a protective manner [9], they contribute to the material removal processes.

The erosion behaviour of the TCS switch electrodes can vary considerably, depending upon the physical and chemical properties of the electrode materials employed. Elkonite displayed the lowest erosion rate of the tested materials, an expected result considering the rigidity of the tungsten matrix at high temperatures. On the other hand, due to its lower melting temperature, copper is slowly drawn out to the surface of the electrodes [13]. As the plasma ionic species interact with the electrode material, mainly copper and tungsten fluorides (CuF/CuF_2, WF_6) as well as smaller quantities of copper and tungsten sulfides (CuS, WS_2) are formed [10, 16, 19]. Copper fluorides, being more volatile, can condense in a lower temperature zone [13] around the rod tip or close to the trigger edge, whilst most of the copper and tungsten sulfides or metallic tungsten can remain fixed on the central discharge areas. The above mechanism explains the observed preferential deposition of fluorine and sulphur compounds on the surfaces of the elkonite electrodes.

An interesting result was the reasonably good performance of aluminum, particularly when its low melting temperature and moderately high reduction strength (reactivity) is considered [10, 16, 19]. A possible explanation for this result could involve the formation of aluminum fluoride (AlF_3), which was detected in large concentrations on the discharge areas of both the rod and trigger disc electrodes. The distribution of this gas-electrode compound indicates that it remains fixed at its formation place, a result of the combination of the high melting temperature of AlF_3 (≈1300 °C), together with the thickness of the gas-electrode reaction zone, which is expected to extend to a considerable depth [18, 20]. From the above, it is suggested that this AlF_3 layer, retards to some extent the erosion process by limiting the removal of electrode material from the discharge areas.

The moderately high erosion rates displayed by the stainless steel rod electrodes (SSt303/SSt316) was expected considering the poor performance of this material in air [9]. Moreover, apart from its poor thermo-physical properties, the chemical affinity of iron for the plasma ionic species play a decisive role on the erosion mechanism [21, 22], as indicated by the high concentrations of iron fluorides (FeF_2/FeF_3) and iron sulfide (FeS) detected on the SSt303/316 electrodes. Additionally, the morphology of the FeF_2/FeF_3 deposits on the rod electrode indicate that these compound formations (Figure 9b) posses poor adhesion properties to the underlying metallic surface

[23], which in turn may further enhance the erosion mechanism.

Finally, in the case of brass, the polarity of the charging voltage was found to have a significant influence on the erosion process, with the positively charged electrodes always displaying much higher erosion rates than the negatively charged electrodes. This polarity effect has been also observed in multi-kHz gas discharge Eximer lasers, where brass electrodes are operated in noble gas - fluoride (KrF/ArF) and molecular fluorine (F_2) atmospheres [24, 25]. From the surface morphology and EDS chemical analysis results this effect can be directly related to the concentrations of gas-electrode compounds detected on the electrode discharge areas. Furthermore, due to the fact that these compounds comprise mainly of copper and zinc fluorides (CuF/CuF_2, ZnF_2), it is suggested that the anode erosion process is enhanced from the large number of negative fluorine ions (F^-) present in the decaying spark plasma column below 5000K [25-27]. Despite the lack of erosion data with a negative charging voltage for the rest of electrode materials used, it is believed that this polarity effect is most prominent with brass [25, 28], where it primarily affects copper, as indicated by its moderate depletion only from the anode electrodes [25].

During the lifetime tests in SF_6, it was observed that the modification of the rod electrode tip as well as the deterioration (poisoning) of the switching gas had an influence on the operational characteristics of the TCS switch. In order to investigate the combined influence of these effects, an additional test was conducted. Figure 16 displays the variation of the breakdown voltage across the TCS switch before and after a typical lifetime test operation cycle (30 seconds at a PRF of 1 kHz). The breakdown levels recorded on the graph were monitored by applying a slowly rising positive voltage across the TCS switch once every minute for a period of 1hour before, and one 1hour and 40 minutes after the 1 kHz test cycle. The first area of this graph (1 hour) is characterized by a small rise of the breakdown voltage levels from 18 to 20 kV, due to the gradual conditioning (pitting) of the polished rod electrode tip with increasing number of switch closures.

Following this conditioning period the switch was operated for 30 seconds at a PRF of 1 kHz (30000 unrecorded shots), after which the breakdown voltage level increased to about 24 kV. This increase, as shown in the second area of Figure 16, is a direct result of the severe rod tip modification and gas deterioration that occurred during high PRF operation. During this period, in which the deteriorated gas was allowed to remain within the switch volume for 1 hour, the breakdown voltage gradually declined with a rate of ~2 kV/hour. This is primarily due to the decay of relatively long lived gas by-products with higher insulating properties than SF_6 [10] produced within the confined switch volume. Finally, when the switch was refilled with new gas (third area) the breakdown voltage dropped to a level of about 22.5 kV with small differences in the appearance of the corona discharge between deteriorated and new gas.

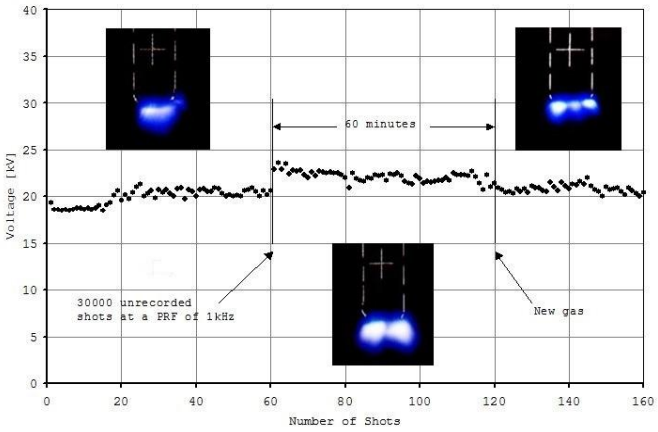

Figure 16. Temporal breakdown voltage behavior of the TCS switch and associated corona discharge appearance before and after a typical lifetime operation cycle of 30000 shots at a PRF of 1kHz with elkonite electrodes.

From this test, it is clear that both the rod electrode modification and switching gas deterioration can influence the operational behaviour of the device, albeit only in a minor way. On the contrary, with synthetic air the combination of these effects resulted in an increased corona discharge activity and accompanied inconsistent switch performance [9]. This difference can be attributed primarily to the highly stable mode of the corona discharge in SF_6, by which the breakdown voltage is only moderately increased despite the heavy modification of the rod electrode, as well as due to the relatively small difference in the dielectric strength between fresh and deteriorated SF_6 gas.

5 CONCLUSIONS

The electrode erosion and lifetime performance of a sealed, rod-plane TCS switch with electrodes made from elkonite (a copper-tungsten composite), two types of stainless steel, brass and aluminum has been investigated. The switch was filled with SF_6 at a pressure of 80 kPa (0.8 bar) absolute, and operated at a repetition rate of 1 kHz. The erosion of the rod electrode was found to play a predominant role on the switch lifetime, with the latter having an inversely proportional relationship to the former. The trigger disc electrodes also provided some information, which was however mainly limited to the various gas-electrode interaction processes occurring during the arc discharge.

Of the five types of rod (anode) electrode materials tested, elkonite exhibited the lowest erosion rate, which consequently resulted in the highest lifetime (0.57×10^6 shots). Despite its poor thermo-physical properties aluminum showed the second best performance after elkonite, whilst the two types of stainless steel electrodes followed closely. Lastly, the brass rod electrode displayed the highest erosion rate with a positive charging voltage, resulting in the worst switch lifetime performance of only 0.2×10^6 shots.

From the results obtained during this study it is evident that the erosion mechanism is dominated by the highly corrosive action of SF_6 ionic decomposition by-products, present in the plasma channel. For some electrode materials tested, the

volatility and poor adhesion properties of metal fluorides and sulfides formed on the discharge regions enhance further the efficiency of the erosion mechanism, thus failing to provide any degree of protection to the underlying metallic surface. A supplementary lifetime test with brass electrodes and a negative charging voltage showed a strong influence of polarity, at least for this material type, with the rod (cathode) erosion rate measured to be lower by a factor of four, whilst that of the trigger disc (anode) increased by about 35%.

Finally, the rod electrode surface modification and switching gas decomposition was found to have a minor influence on the operational consistency of the TCS switch in SF_6. This was attributed primarily to the highly stable corona discharge and to the small alterations of the dielectric strength of SF_6 gas due to sparking.

6 ACKNOWLEDGEMENTS

The authors wish to acknowledge the financial support from the Faculty of Engineering, the Centre for Electrical Power Engineering (CEPE) and the Pulsed Power Group of the University of Strathclyde. The authors would also like to thank Prof. E. V. Hristoforou for his valuable assistance and time allocation at the Scanning Electron Microscopy facility of the Department of Mining Engineering and Metallurgy, National Technical University of Athens.

7 REFERENCES

[1] S. J. MacGregor, S. M. Turnbull, F. A. Tuema and O. Farish, "Factors affecting a methods of improving the pulse repetition frequency of pulsed and dc charged high pressure gas switches", IEEE Trans. Plasma Sci., Vol. 25, pp. 110-17, 1997.

[2] S. J. MacGregor, S. M. Turnbull, F. A. Tuema and O. Farish, "Enhanced spark gap switch recovery using non-linear V/p curves", IEEE Trans. Plasma Sci., Vol. 23**,** pp. 798-804, 1995.

[3] P. Koukos, *"Impulse electrical breakdown and time lags in SF_6"*, University of Strathclyde, Glasgow, UK, MPhil Thesis, 1988.

[4] H. C. Pollock and F. S. Cooper, "The effect of pressure on the positive point-to-plane discharge in N_2, O_2, CO_2, SO_2, SF_6, CCl_2F_2, A, He and H_2", Phys. Rev., Vol. 56, pp. 170-175, 1939.

[5] J. M. Koutsoubis and S. J. MacGregor, "Effect of gas type on high repetition rate performance of a triggered, corona stabilised switch" IEEE Trans. Dielectr. Electr. Insul., Vol. 10, pp. 245-255, 2003.

[6] V. N. Maller and M. S. Naidu, *High Voltage Insulation and Arc Interruption in SF_6 and Vacuum*, Pergamon Press, New York, Ch. 1, 1981.

[7] J. M. Koutsoubis and S. J. MacGregor, "Electrode erosion and lifetime of a triggered corona stabilised switch in SF_6 and air at a repetition rate of 1 kHz", XIII Int'l. Conf. Gas Discharges and their Applications, Vol. 1, pp. 462-465, 2000.

[8] A. L. Donaldson, M. O. Hagler, M. Kristiansen, G. Jackson and L. Hatfield, "Electrode erosion phenomena in high-energy pulsed discharge", IEEE Trans. Plasma Sci., Vol. 12, pp. 28-38, 1984.

[9] J. M. Koutsoubis and S. J. MaGregor, "Electrode erosion and lifetime performance of a high repetition rate, triggered corona stabilised switch in air", J. Phys. D: Appl. Phys., Vol. 33, pp. 1093-1103, 2000.

[10] F. Y. Chu, "SF_6 decomposition in gas-insulated equipment", IEEE Trans. Dielectr. Electr. Insul., Vol. 21, pp. 693-725, 1986.

[11] S. J. MacGregor, J. M. Koutsoubis and S. M. Turnbull, "The design and operation of a compact high-voltage, high pulse repetition frequency trigger generator", Meas. Sci. Technol., Vol. 9, pp**.** 1899-1905, 1998.

[12] J. M. Koutsoubis, S. J. MacGregor and S. M. Turnbull, "Triggered switch performance in SF_6, air and an SF_6/air mixture", IEEE Trans. Plasma Sci., Vol. 27, pp. 272-281, 1999.

[13] L. B Gordon, M. Kristiansen, M. O. Hagler, H. C. Kirbie, R. M. Ness, L. L. Hatfield and J. N. Marx, "Material studies in a high energy spark gap", IEEE Trans. Plasma Sci., Vol. 10, No. 4, pp. 286-293, 1982.

[14] J. A. Bearden, "X-ray wavelengths", Rev. Mod. Phys., Vol. 39, pp. 78-124, 1967.

[15] D. Briggs and M. P. Seah, *Practical Surface Analysis by Auger and X-ray Photoelectron Spectroscopy*, Willey, New York, Ch. 3-5, 1983.

[16] C. Bayer, H. Jenett and D. Klockow, "Influence of reactive SF_6 gases on electrode surfaces after electrical discharges under SF_6 atmosphere", IEEE Trans. Dielectr. Electr. Insul., Vol. 7, pp. 234-240, 2000.

[17] D. R. Airey, P. H. Richards and J. D. Swift, "Time-resolved radial temperature profiles for 10 kA SF_6 arcs", J. Phys. D: Appl. Phys., Vol. 8, pp. 1982-1993, 1975.

[18] I. Sauers, H. W. Ellis and L. G. Christophorou, "Neutral decomposition products in spark breakdown of SF_6", IEEE Trans. Plasma Sci., Vol. 21, pp. 111-120, 1986.

[19] J. Lampe, H. Latour-Slowikowska and J. Slowikowski J, "Study on metal fluoride product formation caused by the electric arc in SF_6", III Int. Symp. on Gaseous Dielectrics, pp. 433-438, 1982.

[20] A. Goldman, M. Goldman, R. S. Sigmond and I. D. Chalmers, "Chemical modifications of aluminium surfaces in SF_6 insulated equipment", VIII Int'l. Conf. Gas Discharges and their Applications, pp. 469-471, 1985.

[21] A. L. Donaldson, M. Kristiansen, H. Krompholz and M. O. Hagler, "Analysis of electrode surface damage in high energy spark gaps", Proc. 5th IEEE Int'l. Pulsed Power Conf., pp. 457-460, 1985.

[22] S. J. MacGregor, G. A. Woolsey, D. B. Ogle and O. Farish, "The influence of electrode-fluorine reactions on corona and glow discharges in SF_6", IEEE Trans. Plasma Sci., Vol. 14, pp. 538-543, 1986.

[23] J. M. Koutsoubis, *"Lifetime performance and operational characteristics of triggered corona stabilised switches"*, University of Strathclyde, Glasgow, UK, Ph.D. Thesis, 2005.

[24] H. Von Bergmann, U. Rebham and U. Stamm, "Design and technology of excimer lasers", *Excimer Laser Technology*, (D. Basting and G. Marowsky Eds.), Springer-Verlag, Berlin, Ch. 4, 2005.

[25] T. S. Dyer, R. G. Morton, W. D. Gillespie and T. D. Steigner, "Anodes for fluorine gas discharge lasers", US Patent Application Publication, 0071178, 2004.

[26] J. D. Yan, M. T. C. Fang, and Q. S. Liu, "Dielectric breakdown of a residual SF_6 plasma at 3000 K under diatomic equilibrium", IEEE Trans. Dielectr. Electr. Insul., Vol. 4, pp. 114-119, 1997.

[27] J. Kopainsky, "Influence of the arc on breakdown phenomena in circuit breakers", *Current Interruption in High-Voltage Networks*, (K. Ragaller Ed.), Plenum Press, New York), pp. 329-354, 1977.

[28] M. Megherbi, A. Goldman and S. J. MacGregor, "Influence of polarity on electrode surface modifications in 200 torr SF_6 coronas", IX Int. Conf. Gas Discharges and their Applications, pp. 219-222, 1988.

John M. Koutsoubis (A'89-M'98) was born in Chalkis, Euboea, Greece in 1965, and received the B.Sc. degree in electrical engineering from the Technological Educational Institute (TEI) of Chalkis, Greece in 1989, and the Ph.D. degree in electronic and electrical engineering from the University of Strathclyde, Glasgow, U.K. in 2005. He has been with TEI of Central Greece in Chalkis, as an Assistant Lecturer since 1992, and elected Lecturer and Senior Lecturer in high-voltage engineering in 2010 and 2015, respectively. From 2000 to 2010, he was additionally employed as a Research Director at the high-voltage and high-current research laboratory of ELEMKO SA in Thebes, Greece. His research interests include high-repetition rate and high-power switching, high-voltage pulse generation, and high-voltage and high-current testing techniques and diagnostics. Dr. Koutsoubis is a member of the IEEE Dielectrics & Electrical Insulation, Nuclear & Plasma Science societies, and of the Scientific Society of Technological Education Engineers (EETEM).

Katerina Thoma (A'88) received the B.Sc. degree in electronic engineering from the Technological Educational Institute (TEI) of Crete (Chania), Greece in 1988. She has been working at the National Technical University of Athens since 1993 as a Special Technical Staff in Scanning Electron Microscopy, at the Laboratory of Physical Metallurgy, and from 2002 till today she works as a Special Laboratory Teaching Staff and S.E.M specialist at the same Laboratory. She is also member of the Scientific Society of Technological Education Engineers (EETEM).

Scott J. MacGregor (M'95) received the B.Sc. and Ph.D. degrees from the University of Strathclyde, Glasgow, U.K., in 1982 and 1986, respectively. He is currently with the University of Strathclyde, where he became a Pulsed Power Research Fellow in 1986, a Lecturer in pulsed-power technology in 1989, a Senior Lecturer in 1994, and a Reader and a Professor of high-voltage engineering in 1999 and 2001, respectively. He has been Dean of Engineering at the University of Strathclyde since 2010. His research interests include high-voltage pulse generation, high-frequency diagnostics, high-power repetitive switching, high-speed switching, electronic methods for food pasteurization and sterilization, generation of high-power ultrasound (HPU), plasma channel drilling, pulsed-plasma cleaning of pipes, and stimulation of oil wells with HPU.